Interaction and Complexation of Phospholipid Vesicles and Triblock Copolymers

Yu Yuan Chieng and Shing Bor Chen*

Department of Chemical and Biomolecular Engineering, National University of Singapore, Singapore 117576

Received: July 21, 2009; Revised Manuscript Received: September 14, 2009

Mixtures of Pluronic (F-127 or L-61) and phospholipid were investigated for a wide range of Pluronic concentrations (0−15 wt %) using dynamic light scattering, differential scanning calorimetry, and fluorescence microscopy. The present study is aimed at better understanding how the amphiphilic triblock copolymers affect the lipid vesicles, particularly in the high-concentration regime. Our results show that L-61 interacts more strongly with phospholipid vesicles than F-127 when the copolymer is at the unimer state in the solution. For high concentrations, F-127 forms mixed micelles with solubilized lipid molecules in the form of bilayer patches. This novel behavior was observed for the first time. In contrast, more hydrophobic L-61 tends to precipitate with the solubilized lipids as large crew-cut mixed aggregates.

1. Introduction

Phospholipid vesicles have been studied extensively since the 1960s due to their diverse applications, mainly in pharmaceuticals. They are good biodegradable carriers as well as biocompatible models for mimicking biological membranes because of their proper size, composition, bilayer fluidity, large internal volume, and wide solubility range.[1−6] Physical stability, encapsulation capacity, sustainable release rate, good bioadhesivity, and thermosensitivity are some of the crucial characteristics for controlling the efficiency of vesicle in vivo performances. To date, although promising results have been obtained from polymer-modified phospholipid vesicle systems, these characteristics have not yet been achieved with great success. A typical polymer-modified lipid system, such as adding polyethylene glycol, usually shows nonthermosensitive and poor adhesive properties for the delivery of drugs to a target site. The polymer may even cause aggregation and fusion of cell membranes.[7−12] To overcome this problem, researchers have targeted the amphiphilic triblock copolymer, also well-known as Poloxamer or Pluronic, as a promising thermosensitive stabilizer.

Pluronic, which exhibits nonionic surfactant properties, has been widely exploited in a number of biomedical applications.[13,14] The copolymer molecules dissolve and exist as unimers in a dilute aqueous solution at low temperature. However, they will self-assemble to form micelles, each having a hydrophobic core surrounded by a hydrophilic corona, when the critical micellization concentration is reached at a given temperature. The hydrophobic core serves as a compartment for the incorporation of hydrophobic compounds, while the hydrophilic corona acts as a stabilizer for the hydrophobic core. The micelle shape and size depend on the copolymer concentration, block lengths, and temperature. Due to the amphiphilicity, the triblock copolymer is sensitive and able to alter the phospholipid membrane properties in response to changes of physical and environmental parameters.

Most of the work in the literature investigated the interaction of phospholipid vesicles with Pluronic at low concentration and yielded rather diverging findings.[15−20] While some studies reported negative effects, such as a high rate of encapsulated material leakage and a shorter blood circulation time,[21,22] Liang et al.[23] found that Pluronic not only provides good stealth stabilization to the liposomes but also enhances the micromechanical properties of the bilayer. Comparatively, scarce literature is available for the interaction between vesicles and Pluronic at a micellar state or a gel state, even though the mixture shows promising results in enhancing the sustained release rate and strengthening material microstructure.[24,25]

Apart from acting as a vesicle stabilizer, amphiphilic triblock copolymer alone has also been investigated to optimize drug and gene delivery systems.[26−32] Micelle-based formulation of SP1049C developed by Kabanov's group is a successful example of drug delivery systems for chemotherapeutic treatment.[33,34] The formulation consists of Doxorubicin and Pluronic mixture, which is a combination of Pluronic L-61 and F-127 in a weight ratio of 1:8. SP1049C has now entered the stage of clinical trial II evaluation, and the test data show its ability to hypersensitize multidrug resistant tumor cells.[35,36] In this application, interactions between lipid vesicles and Pluronic are also relevant and essential because the vesicles can act as model cell membranes.

For biological cell membranes, there exist considerable studies on their interaction behavior with Pluronic. Pluronic L-61, compared with many other triblock copolymers, has demonstrated better chemosensitizing effects and is more active in the interactions with multidrug-resistant (MDR) cancer cells.[37,38] L-61 also revealed higher potency in inducing drug Rhodamine 123 accumulations in MDR cells compared to F-127.[39] In addition, Krylova et al. found that adsorption of Pluronics on membranes induced disturbance to the lipid packing.[40] Nineteen different amphiphilic triblock copolymers have been selected and studied mainly using flip-flop measurement in an attempt to uncover their abilities to interact with membranes. L-61 was found to accelerate the flip-flop and increase the permeability of Doxorubicin into the vesicles,[41] suggesting that copolymer hydrophobicity and chemical structure is the main factor determining the disturbance propensity. Similar behavior was also reported by Erukova et al., where more hydrophobic Pluronics L-61 and P-85 caused more pronounced changes in flux and faster solute permeation across the bilayer than more hydrophilic F-68.[42] Despite the great advantages, the drawback of L-61 is its low solubility and critical micellization concentra-

* To whom correspondence should be addressed. Tel.: (65) 6516 5237. Fax: (65) 6779 1936. E-mail: checsb@nus.edu.sg.

10.1021/jp906929u CCC: $40.75
Published on Web 10/16/2009

tion, constraining the solution preparation at effective concentrations for optimum drug transportation. The effect of Pluronic (F-127, P-85, and L-61) as a drug carrier on the cytotoxicity of carboplatin to rat cell lines has been investigated by Exner et al.[43] They found that Pluronic P-85 has the most potent sensitizing effect on enhancing the toxicity of carboplatin. L61 was toxic to cells, while F-127 shows its ability to stimulate cell viability and proliferation. Nevertheless, detailed interaction mechanisms between cell membranes and copolymers remain unclear for the interesting change in the enhancement of carboplatin toxicity to the cell membranes.

In view of the advantages of L-61 and F-127 for pharmaceutical applications, it is critically important to gain a fundamental understanding of how they interact with phospholipid membranes. Since F-127 and L61 have quite different length ratios of hydrophilic to hydrophobic block, they are expected to affect phospholipid vesicles differently at the molecular level. To the best of our knowledge, interactions of lipids with F-127 and L-61 spanning a wide range of concentrations are not yet fully explored. In this study, we aim to experimentally investigate and elucidate the interaction mechanisms for the mixture of phospholipid and Pluronic using different characterization methods. The obtained results will shed light on the design of a phospholipid−copolymer system with desired stability and sensitivity.

2. Experimental Section

Materials. Pluronic F-127 ($PEO_{100}-PPO_{65}-PEO_{100}$) with hydrophilic to lipophilic balance (HLB) = 22 and L-61 ($PEO_2-PPO_{30}-PEO_2$) with HLB = 3 from BASF Corporation with average molecular weight of 12 600 g/mol and 1950 g/mol, respectively, were used in this study as received. They were selected based on their different properties such as molecular weights, lengths of PEO and PPO blocks, hydrophilicity, and critical micelle concentration. L-α phosphatidylcholine (egg PC) and 1,2-dipalmitoyl-*sn*-glycero-3-phosphocholine (DPPC) with ≥99% purity from Sigma-Aldrich (Singapore) were used to prepare phospholipid vesicles. High-purity sodium chloride (BDH Anala), chloroform (analytical reagent grade), and methanol (ACS grade) were purchased from Merck. Tetrahydrofuran (HPLC 99.8% purity) was obtained from Tedia, USA. 1,6-Diphenyl-1,3,5-hexatriene (DPH) for fluorescence with ≥97.5% purity was from Fluka. Deionized water with a resistivity of 18.2 MΩcm was obtained from a PureLab Maxima water purification system (ELGA). All glassware was cleaned and rinsed thoroughly with deionized water prior to use.

Preparation of Pluronic Solution. Pluronic F-127 solutions ranging from 0.02 to 15 wt % and 0.02 to 0.5 wt % for L-61 solutions were prepared at room temperature. This concentration range was selected due to the convenience of F-127 preparation at room temperature without using the cold method as described by Schmolka (1977).[44] Deionized water or 20 mM NaCl buffer solution was slowly added to a weighed amount of Pluronic, and the sample was then gently stirred for 12 h. For 0.7−15 wt % L-61, the solutions are turbid at room temperature or higher. Therefore, these solutions were prepared and stirred in an ice bath to ensure complete dissolution of L-61. The dissolved Pluronic solutions were then allowed to undergo hydration and dispersion overnight at 4 °C in a refrigerator. All samples were brought to room temperature before use.

Preparation of Phospholipid Vesicles−Pluronic Solution. Phospholipid vesicles were prepared based on the conventional thin-film hydration method. An appropriate amount of phosphatidylcholine lipid was dissolved in chloroform/methanol with a volume ratio of 2:1. The solvent was thoroughly evaporated to dryness in a water bath under continuous flow of nitrogen. The dry lipid film formed in the bottom flask was then resuspended in an aqueous buffer solution (20 mM NaCl) with and without Pluronic. Samples were vortexed several times until all the lipid molecules were well dispersed and homogenized in a water bath at a temperature above the main phase transition temperature of the lipid (−15 to −5 °C for egg PC and 41 °C for DPPC) for 2 h. The final lipid concentration of the prepared samples was fixed at 0.5 mg/mL unless otherwise stated. To obtain unilamellar vesicles, we sonicated multilamellar vesicles in a bath sonicator and centrifuged the sample, 1 h for each process.

Dynamic Light Scattering (DLS). The average hydrodynamic diameter and size distribution of each unilamellar vesicle sample were determined using a Brookhaven 90 Plus particle size analyzer at 90° scattering angle. A semiconductor laser diode (30 mW) is the light source with wavelength of 659 nm. Prior to measurements, samples were extruded and filtered through a polycarbonate membrane of 0.2 μm pore size. All measurements were made at 25 °C. The low vesicle concentration of 0.5 mg/mL and Pluronic concentrations from 0.02 to 1 wt % were used to ensure negligible multiple scattering. Data fitting and analysis were conducted based on the CONTIN method. The measurements were repeated at least 5 times to take an average for each sample.

Fluorescence. Hydrophobic dye, DPH (λ_{ex} = 350 nm/λ_{em} = 428 nm), was used as the fluorescent probe in our study. Fluorescence experiments were carried out using a Leica fluorescence microscope (DMLM microscope, Germany) equipped with a mercury lamp (ebq 100 isolated). A filter cube (type A) suitable for DPH was used for excitation between 340 and 380 nm and emission above 400 nm. The molar ratio of lipid to DPH was kept constant at 100:1 for all preparations. To incorporate DPH into the lipid bilayer, an appropriate amount of DPH was dissolved in tetrahydrofuran and dried together with phospholipids (chloroform:methanol, 2:1) under continuous flow of nitrogen. All procedures were performed in the dark at all times. Each sample solution was pipetted onto a microscope slide, which was then covered with a glass coverslip (22 mm × 22 mm, thickness 0.13−0.17 mm) before analysis on the microscope using the reflected mode of observation. All experiments were conducted at least twice at 25 °C to check the reproducibility.

Differential Scanning Calorimetry (DSC). DSC experiments were performed using a Mettler Toledo DSC822 differential scanning calorimeter. An aluminum sealed pan (40 μL) was filled with approximately 10 mg of sample solution, while an empty pan was used as the reference. The data were collected in a heating, cooling, and heating thermal cycle from −10 to 60 °C at a scan rate of 2.5 °C/min. For analysis and comparison purposes, DSC curves at the second heating run were used to eliminate the influence of thermal history. All measurements were repeated three times for each sample with high reproducibility within ± 0.1 °C.

3. Results and Discussion

DLS for the Unilamellar Vesicle/Pluronic System. ***(a) F-127.*** For pure F-127 in the absence of vesicles, the critical micellization concentration (CMC) at 25 °C has been reported to be around 0.7% w/v.[45] Our DLS experiment at 25 °C found that reliable results for the hydrodynamic diameter could be obtained with high enough average count rates only when the F-127 concentration was 0.5 wt % or higher. At 0.5 wt % F-127,

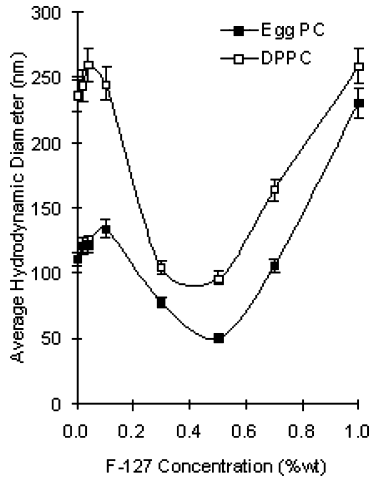

Figure 1. Hydrodynamic diameter of large unilamellar vesicles with addition of F-127.

the measured size distribution spans from 1 to 26 nm, with the average hydrodynamic diameter being around 5.4 nm, implying that most of the F-127 molecules still existed as unimers in the solution. When the concentration was raised to 0.7−1.0 wt %, micelles formed, and the average hydrodynamic diameter was increased to around 20 nm. All of the F-127 solutions showed a high polydispersity (>0.4). The micellization of F-127 can also be detected by DSC as will be discussed later.

In the absence of Pluronic, we obtained large unilamellar vesicles (0.5 mg/mL) from egg PC and DPPC with average hydrodynamic diameter equal to 111 and 236 nm, respectively. The sizes are comparable with those (100−250 nm) reported in the literature also using the thin-film hydration method.[36,46,47] For vesicles and F-127 mixtures, Figure 1 plots the average hydrodynamic diameter versus F-127 concentration. Note that the DLS experiments showed a high reproducibility with the deviation within 5% of the average diameter. For both lipids, we found that the vesicle size increased with the added amount of F-127 in the low concentration regime. A further increase in the F-127 concentration led to a decrease in the hydrodynamic diameter until the concentration reached about 0.5 wt %, which is close to the F-127 CMC without lipid. At higher concentrations (0.7−1.0 wt %), the hydrodynamic diameter increased again with F-127 concentration. The size distributions for egg PC/F-127 at four F-127 concentrations are shown in Figure 2.

At low enough concentrations, F-127 molecules exist as unimers, and their hydrophobic blocks (PPO) can be inserted into the lipid bilayer, leading to bilayer expansion, according to the work of Liang et al. from atomic force microscopy characterization.[23] The two PEO blocks of each F-127 molecule dangle at the different sides in the outside of bilayer, partially accounting for the vesicle size increase. Liang et al. also reported a considerable increase in the measured membrane bending modulus due to the addition of Pluronic. The improved bending rigidity is the main mechanism for the observed vesicle size increase. In our study, the incorporation is also supported by the similar single broad peak in the absence and presence of F-127 (cf. Figure 2a and 2b), except for the shift to larger sizes. DPPC is a synthetic phospholipid with fully saturated aliphatic chains, as opposed to egg PC (natural phospholipid) with a partly unsaturated chain. Due to their structure with a weaker packing order, egg PC vesicles are thought to have a higher incorporation loading of additives than DPPC vesicles.[48] For 0.04 wt % F-127, we found that the size increment for DPPC vesicles is 26 nm when compared to 12 nm for egg PC vesicles. It should be noted that the membranes of egg PC vesicles show fluidity at room temperature due to the low main phase transition temperature (−15 to 5 °C). Incorporation of Pluronic PPO chains in their liquid-phase bilayer may not increase the bending rigidity as much as for DPPC, and hence a smaller vesicle size increase results. According to the cryo-TEM micrographs obtained by Johnsson et al.,[49] F-127 appears to show stronger interaction with larger-size vesicles, resulting in the formation of a small number of bilayer disks and corresponding open vesicles that coexist with the remaining F-127 incorporating vesicles of smaller sizes. At low concentration, the solution was dominated by the intact vesicles with incorporated F-127, thus we observed an increase in the average hydrodynamic diameter. Beyond this low concentration regime, the decrease in hydrodynamic diameter with increasing F-127 concentration can be explained by the solubilization process. Most of the large unilamellar vesicles were destructed, yielding many bilayer disks of much smaller sizes in coexistence with small F-127 modified unilamellar vesicles that are enlarged only moderately. Therefore, the average hydrodynamic diameter at 0.3 wt % was reduced. This behavior persisted until the F-127 concentration reached about 0.5 wt %. The presence of lipids may likely cause F-127 to undergo micellization at a concentration slightly lower than 0.7 wt %, the CMC for pure F-127 at 25 °C. The micellizing F-127 can further facilitate the solubilization of smaller vesicles by taking up bilayer disks for the formation of mixed micelles. As can be seen from Figure 2c, the size distribution has become bimodal, and the sample also showed a decreased turbidity and light scattering intensity, all clearly indicative of the existence of entities with small sizes: mixed micelles, bilayer disks, and small vesicles. A similar trend for vesicle size decrease was reported for addition of several nonionic surfactants.[50−52] At higher concentrations of 0.7−1.0 wt %, the population of mixed micelles grew considerably, while the vesicles and bilayer disks were reduced in number because of substantial solubilization. The existence of a small number of Pluronic modified vesicles at these high concentrations of F-127 (equivalent to 45−55 mol %) was already evidenced from the cryo-TEM micrograph at 50 mol % of F-127.[42] These mixed micelles might grow or even complex with irregular and curved bilayers from disrupted vesicles, leading to the increase of the average hydrodynamic diameter.[50] In other words, Pluronic F-127 may not be able to completely solubilize the vesicles for concentrations up to 1.0 wt %. To make a comparison with the Lichtenberg three-stage model for the effect of addition of nonionic surfactant,[53−57] we tested egg PC vesicles by adding Triton X-100 and did observe a size increase followed by a decrease before the CMC, and then leveling off when the surfactant concentration was progressively increased. Unlike the case of F-127, there was no subsequent size increase.

(b) L-61. L-61 has very different physical properties from F-127 regarding the molecular weight, block lengths, hydrophilic to lipophilic balance (HLB = 3), and microstructure of micelles. F-127 with a higher HLB at 22 and molecular weight tends to form star-type spherical micelles in a wide range of concentrations. In contrast, more hydrophobic L-61 will form condensed crew-cut aggregates coexisting with unimers, rather than spherical micelles even at low concentration and temperature.[58] According to the literature, L-61 will form aggregates when the concentration exceeds the CMC (1.1×10^{-4} M or 0.022 wt % at 25 °C).[34] For pure L-61 at 0.04−0.1 wt %, our DLS found the average hydrodynamic diameter of the aggregates to be 260 nm, which is comparable to that of large unilamellar DPPC vesicles (236 nm) without L-61. By further increasing L-61

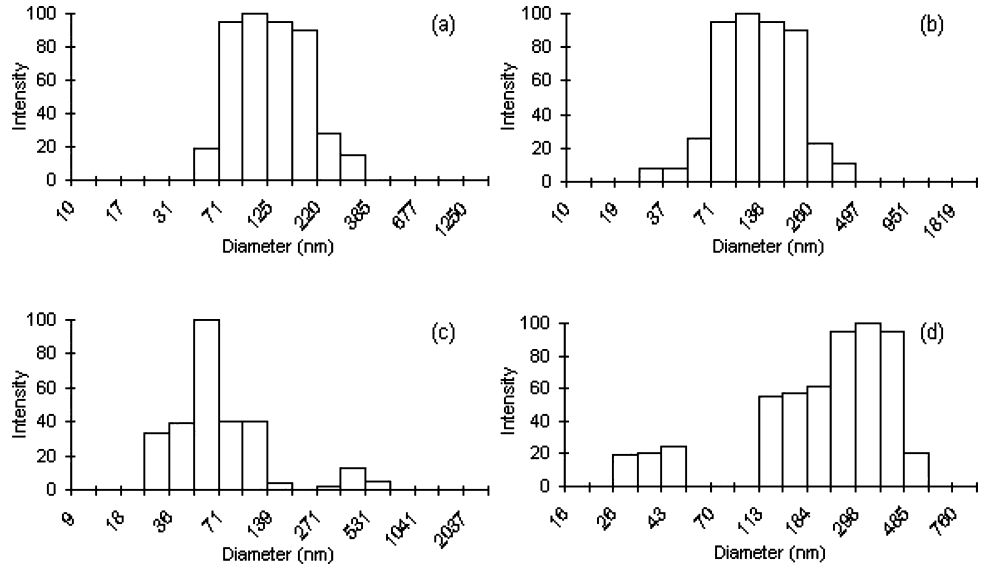

Figure 2. Size distribution of egg PC vesicles with varying concentration of F-127.

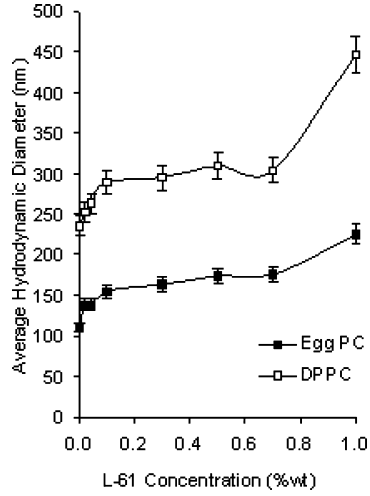

Figure 3. Hydrodynamic diameter of large unilamellar vesicles with addition of L-61.

concentration, the hydrodynamic diameter was increased, implying the agglomeration of crew-cut L-61 aggregates. At room temperature, the L-61 solution at 0.7 wt % or above was already cloudy.

For lipid/L-61 mixtures, we plot the average hydrodynamic diameter against L-61 concentration in Figure 3. It has to be pointed out that at the lowest concentration of L-61 (0.02 wt %), very large, visible aggregates formed and coexisted with modified vesicles. These large aggregates could not be analyzed and were indeed removed by centrifugation and filtration using 0.2 μm polycarbonate membranes before DLS characterization. The reason for the formation of the large aggregates is unknown at this concentration, which is slightly lower than CMC for pure L-61. Excluding this special case, one can see from Figure 3 that the hydrodynamic diameter increases with increasing L-61 concentration for the concentration range investigated. This behavior was also observed by Kostarelos et al. for low concentrations of L-61.[15] Similar to F-127, the PPO of L-61 molecules can be inserted in the lipid bilayer, but their very short dangling PEO at both sides of the bilayer definitely cannot account for the observed size increase. Liang et al. claimed that hydrophobic PPO exhibits a more significant effect on the vesicles size than PEO, due to the bilayer expansion during PPO incorporation.[23] In their study, Pluronic L-81 ($PEO_2-PPO_{40}-PEO_2$, with HLB = 2), which is very similar to L-61, also caused a size increment comparable to that by F-127 at 0.02 wt %. This behavior is again attributable to enhanced bending rigidity. Above CMC, L-61 solubilized lipid molecules considerably, leading to formation of mixed aggregates. The size increase becomes less pronounced in the concentration range 0.1−0.7 wt %. Unlike the F-127 cases, we are unable to judge whether mixed aggregates and vesicles coexist from DLS because (1) the aggregates of pure L-61 do not differ much from DPPC vesicles in size and (2) the obtained size distribution is broad without a clear bipeak in most cases.

DSC and Fluorescence Microscopy for Multilamellar Vesicle/Pluronic System. To further investigate the effect of Pluronic spanning from a low to high concentration, we applied DSC and fluorescence microscopy for multilamellar vesicles. For DSC studies, researchers prefer multilamellar vesicles to unilamellar vesicles because the latter obtained by sonication has a high surface curvature (small radius) and will show a broad peak for the phase transition.[4,59] Regardless of the number of bilayers in a vesicle, the nature of interaction with Pluronic should be essentially the same. Hence, the behavior inferred from DSC and fluorescence might still be qualitatively compared with that from DLS.[60] The dye used in fluorescence microscopy is 1,6-diphenyl-1,3,5-hexatriene (DPH), which will show fluorescence intensity when bound and localized between the acyl chains of lipid molecules through hydrophobic interaction. This hydrophobic fluorescent probe enables direct visualization of multilamellar vesicles under a microscope because they are large enough. For DSC, DPPC is appropriate since the vesicle's transition from a gel to a liquid crystalline phase takes place sharply at about 41 °C. For egg PC, however, the transition temperature is much lower spanning a certain range (−15 to −5 °C) due to the heterogeneous nature of the lipid having both saturated and unsaturated hydrocarbon chains.[4,60,61] As such, we used DPPC multilamellar vesicles to do the experiments. For validation, DSC characterization for 50 mg/mL of DPPC without Pluronic was first attempted, showing a pretransition temperature at 36 °C and a sharp main phase transition temperature $T_m \sim$ 41 °C, in good agreement with prior studies.[62−64] To facilitate comparison, the DPPC concentration was kept at 0.5 mg/mL in the DSC study, which is the same as the value for DLS, although the vesicles were no longer unilamellar. At this lower

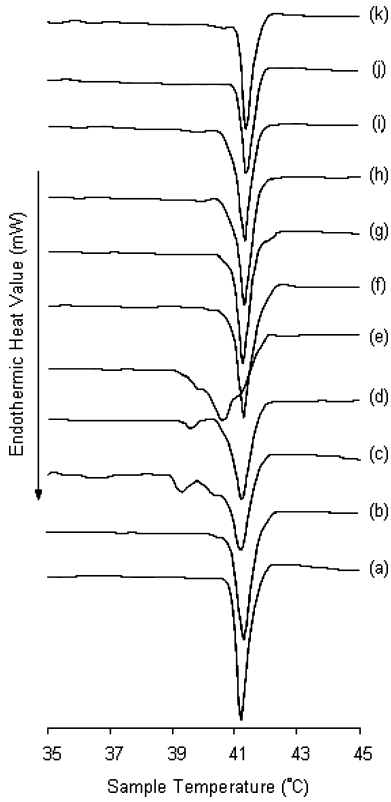

Figure 4. DSC thermogram of DPPC vesicles at different F-127 concentrations: (a) 0.0; (b) 0.02; (c) 0.04; (d) 0.1; (e) 0.3; (f) 0.5; (g) 0.7; (h) 1.0; (i) 5.0; (j) 10.0; and (k) 15.0 wt %.

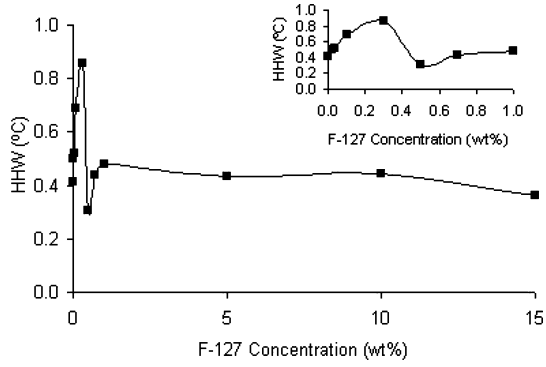

Figure 5. HHW of the main phase transition peak vs F-127 concentration (0−15 wt %). The inset is an enlarged plot for low concentrations.

lipid concentration, only the main phase transition temperature could be detected.

(a) F-127. Figure 4 shows the DSC results at various concentrations of added F-127. We found that the addition of F-127 to vesicles could only cause a very weak shift of the main phase transition temperature, implying that the lipid bilayer structure somehow remained. The half-height width (HHW) of the peak is shown in Figure 5, while the transition enthalpy change (ΔH, endothermic) is presented in Table 1. Also shown in the table is the peak value of F-127 micellization temperature (CMT), if detectable. HHW is an indicator for the interaction between added compounds and the phospholipid bilayer. In principle, the HHW of the main transition peak will increase with increasing strength of the molecular interaction (peak broadening). One can see from Figure 4 that at 0.02−0.30 wt % F-127 results in decreased T_m and peak broadening. This effect becomes stronger with increasing F-127 concentration.

TABLE 1: Thermal Data for DPPC Vesicles Modified by F-127

concentration F-127 (wt %)	ΔH (J/g)	CMT[a] (°C)
0.00	26.1×10^{-3}	-
0.02	23.2×10^{-3}	-
0.04	21.0×10^{-3}	-
0.10	18.9×10^{-3}	-
0.30	25.3×10^{-3}	-
0.50	22.8×10^{-3}	29.3
0.70	19.3×10^{-3}	28.2
1.00	19.2×10^{-3}	26.8
5.00	17.6×10^{-3}	23.5
10.0	14.0×10^{-3}	20.4
15.0	14.1×10^{-3}	17.1

[a] Critical micellization temperature.

At low concentrations, the observed behavior can be explained by incorporation of F-127 unimers into the lipid bilayer. These unimers act as spacers in the lipid bilayer and lower the van der Waals force between lipid hydrocarbon chains, leading to a destabilization effect on the lipids. As a result, the hydrocarbon chains can be disturbed more easily by the thermal energy, and the liquid crystalline state can therefore be reached at a lower temperature with a smaller enthalpy change. In addition, the broadening of T_m peak reveals a lower cooperativity between the acyl chains for the transition. As shown in Figure 5, HHW reaches its maximum of 0.85 °C at 0.3 wt % F-127, indicative of a comparatively strong interaction between DPPC and incorporated F127. For this case, the insertion of F-127 was very significant, while vesicle solubilization was also ongoing. More bilayer disks were detaching from the vesicles, probably accounting for the slight increase of ΔH at 0.3 wt % and the minimum HHW at 0.5 wt %. When the concentration reached or exceeded 0.5 wt %, DSC also detected a very broad CMT peak. The peak location depends on the F-127 concentration but is always lower than T_m as shown in Table 1. For these cases, it means that before the sample temperature was raised to near T_m considerable lipid solubilization and formation of mixed micelles had occurred. Interestingly, when the F-127 concentration was increased from 0.5 to 1.0 wt %, the location and HHW of the T_m peak appeared to be changing back to those in the absence of F-127 (see Figures 4 and 5). This behavior is attributable to the uptake of solubilized lipid by F-127 to form mixed micelles. Each mixed micelle is thought to contain a certain portion of lipid molecules in the form of bilayer patches surrounded by self-assembled F-127 molecules.

This argument is further supported by the observation for the cases with higher concentrations (5−15 wt %), where most of the vesicles were solubilized by F-127 and mixed micelles dominated. The detected main peak is still very similar to that in the absence of F-127, with respect to the peak location and HHW. As shown in Figure 5, HHW almost remains constant from 5 to 15 wt %, whereas the transition enthalpy decreases and tends to level off at 15 wt % (Table 1). The weak variation of HHW indicates minimal interference from F-127 for each of the bilayer patches in the mixed micelles. With increasing F-127 concentration, the number of mixed micelles should increase, and each mixed micelle will contain fewer lipid molecules since the lipid concentration has been fixed at 0.5 mg/mL. We speculate that the number of lipid molecules (not involved in the bilayer patches, but mingled with F-127 in the mixed micelles) increases with F-127 concentration and approaches a constant at high F-127 concentrations. These lipid molecules do not participate in the main phase transition, thereby accounting for the decrease of ΔH (J/g) with increasing F-127

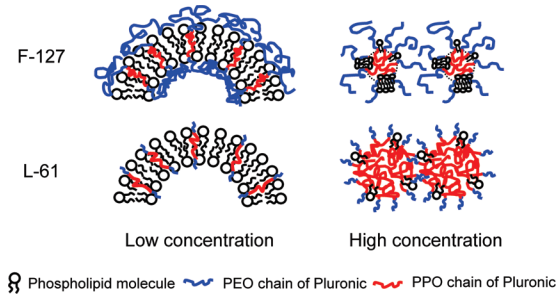

Figure 6. Schematic diagram of interaction and complexation of phospholipid with F-127 and L-61 at low and high concentrations.

concentration toward a constant at 15 wt % F-127. In brief, the interaction and complexation of phospholipid with Pluronic F-127 at low and high concentrations is summarized schematically in Figure 6. It is interesting to compare this behavior to that for a DPPD vesicular solution with added Triton X-100. We tested four surfactant concentrations (0.005, 0.02, 0.5, and 1 wt %) and found that the main transition peak was detectable only for 0.005 wt % (<CMC, 0.015 wt %) and also became broader. Unlike F-127, Triton X-100 at high concentrations solubilized the vesicles without bilayer structure remaining.

To our best knowledge, the main peak restoration at very high F-127 concentrations (5−15 wt %) is reported for the first time in the present study. This result shows the ability of solubilized lipid molecules to maintain a bilayer structure in the mixed micelles. It should be noted that F-127 at sufficiently high concentrations (e.g., 15 wt %) would undergo thermal gelation at about 35 °C. The gel formation appears not to affect the main phase transition of the lipid. This finding is very encouraging as Pluronic improved thermal sensitivity may find applications in the field of pharmaceuticals.

To seek more clues and evidence, we applied fluorescence microscopy and show the images for various F-127 concentrations in Figure 7. Note that for pure F-127 with concentration up to 15 wt % the image was always dark without any DPH intensity. A comparison between Figure 7a for the absence of F-127 and Figure 7b for 0.02 wt % F-127 finds that the presence of F-127 leads to an increase in the number of the fluorescent spots representing vesicles. The enhanced number in vesicles can be explained by the smaller number of bilayers for each of the multilamellar vesicles because the steric effect of the dangling PEO blocks of F-127 can hamper the formation of vesicles with a large number of bilayers. Due to the limitation of size resolution in microscopy, a direct comparison with DLS for the trend of size change is difficult. At 0.3 and 0.7 wt %, the number of vesicles was decreased considerably, reflecting the solubilization of lipid vesicles by F-127. Owing to the broad CMT peak detected at 0.7 wt %, the micellization might have started at room temperature for our fluorescence experiment. Although the bilayer disks and patches could accommodate DPH, they are too small to be seen under the microscopy. This behavior remained at higher F-127 concentrations as shown in Figure 7e and 7f. At 15 wt %, we had hardly seen any fluorescent spots, although the image is not shown here.

One may wonder whether the detected T_m for high enough F-127 concentrations is just due to the existence of some unsolubilized vesicles, and there is no bilayer structure in the mixed micelles. This scenario would have led to a noticeably different HHW, much smaller ΔH, and probably detectable fluorescence at 15 wt % F-127, because the strong solubilization can substantially reduce the number of unsolubilized vesicles, in which F127 is also considerably incorporated. However, our experimental observations suggest otherwise.

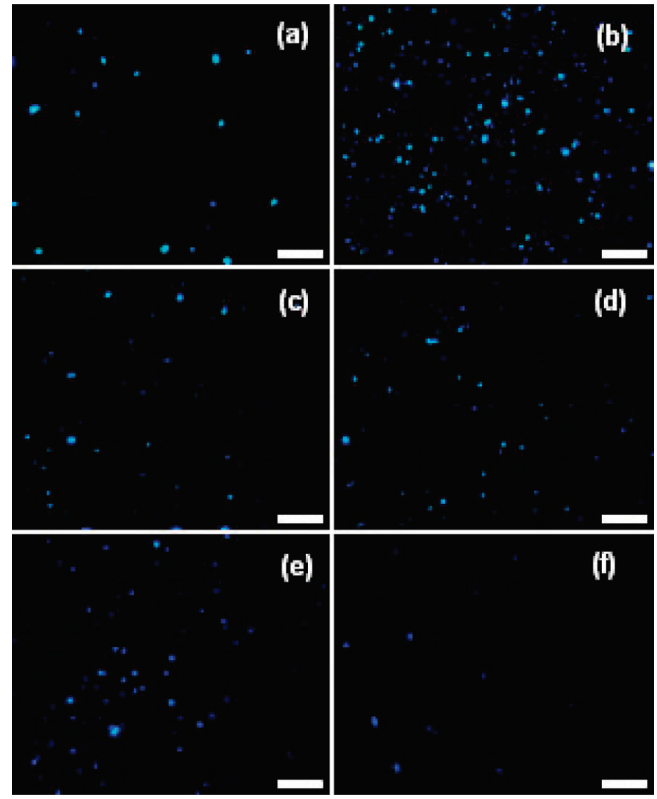

Figure 7. Fluorescence image of DPPC vesicles at different F-127 concentrations: (a) 0.0; (b) 0.02; (c) 0.3; (d) 0.7; (e) 5.0; and (f) 10.0 wt %. Bar = 100 μm. Magnification = 200.

(b) L-61. L-61 has a higher hydrophobic-to-hydrophilic block ratio with hydrophilic blocks much shorter than those of Pluronic F-127. It is known that L-61 can easily form large-size lamellar aggregates with low stability even at low concentrations.[35] As mentioned earlier, the solubility of L-61 at 0.7 wt % is decreased considerably because of the sample's cloudy appearance. A further increase in the concentration above 1 wt % led to flakes precipitated at the bottom of flasks. The effect of L-61 on the DPPC lipid bilayer is presented as a DSC endotherm in Figure 8. The corresponding HHW, CMT, and ΔH are shown in Figure 9 and Table 2, respectively.

Once again, addition of L-61 at the very low concentration of 0.02 wt % induced strong aggregation, similar to what happened to the unilamellar vesicles mentioned earlier. The visible solid complexes formed are responsible for significant peak broadening and an abrupt, significant increase in T_m and ΔH (see curve b of Figure 8). However, upon increasing the concentration to 0.04−0.1 wt % (above CMC), the large solid complexes no longer appeared due to stronger solubilization. The main phase transition peak broadened and shifted to a lower temperature (about 2 °C decrease), while ΔH was slightly larger when compared to the L-61 free counterpart. Compared to F-127, more hydrophobic L-61 can penetrate and disturb the bilayer structure to a greater extent. This argument is supported by the finding of Chang et al. that L-61 shows a stronger penetration ability into a DPPC monolayer at an air−water interface than more hydrophilic F-68.[65,66]

When the L-61 concentration was increased to 0.3 wt % or above, CMT could be detected, as shown in Table 2. The micellization can span a wide temperature range (greater than 20 °C). In the concentration range of 0.3−0.7 wt %, ΔH decreases with the L-61 concentration, while HHW hardly varies. Compared to the case of 0.1 wt %, ΔH drops consider-

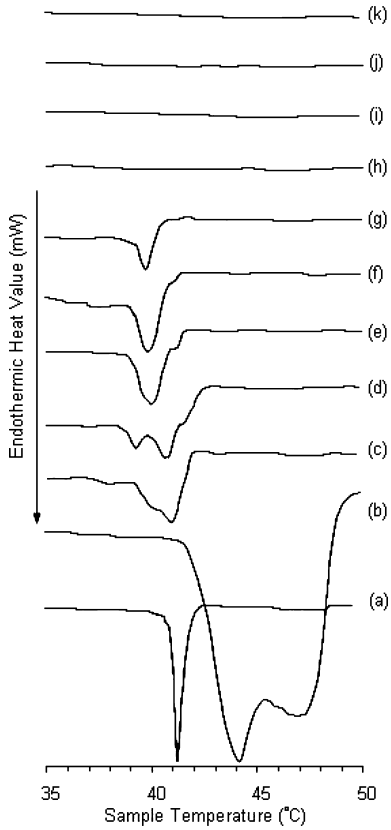

Figure 8. DSC thermogram of DPPC vesicles at different L-61 concentrations: (a) 0.0; (b) 0.02; (c) 0.04; (d) 0.1; (e) 0.3; (f) 0.5; (g) 0.7; (h) 1.0; (i) 5.0; (j) 10.0; and (k) 15.0 wt %.

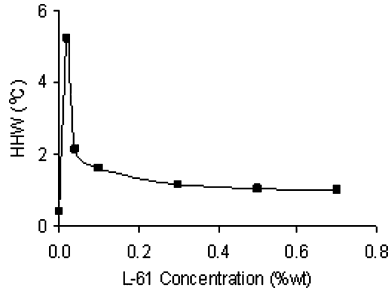

Figure 9. HHW of the main phase transition temperature vs L-61 concentration (0.0−0.7 wt %).

TABLE 2: Thermal Data for DPPC Vesicles Modified by L-61

concentration L-61 (wt%)	ΔH (J/g)	CMT[a] (°C)
0.00	26.1×10^{-3}	-
0.02	0.8	-
0.04	27.6×10^{-3}	-
0.10	27.4×10^{-3}	-
0.30	17.0×10^{-3}	27.6
0.50	16.9×10^{-3}	27.3
0.70	12.1×10^{-3}	27.1
1.00	-	26.8
5.00	-	24.3
10.0	-	22.9
15.0	-	21.5

[a] Critical micellization temperature.

ably, signifying disruption of the lipid bilayers during the solubilization process. The larger reduction in T_m and larger HHW for L-61 than for F-127 indicates that L-61 can disturb and solubilize vesicles more strongly.

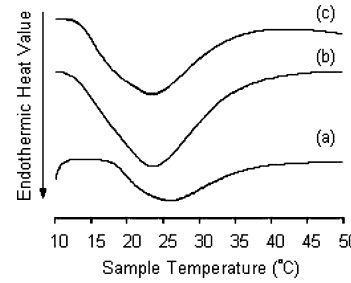

Figure 10. Critical micellization temperature of DPPC vesicles at different L-61 concentrations: (a) 5.0; (b) 10.0; and (c) 15.0 wt %.

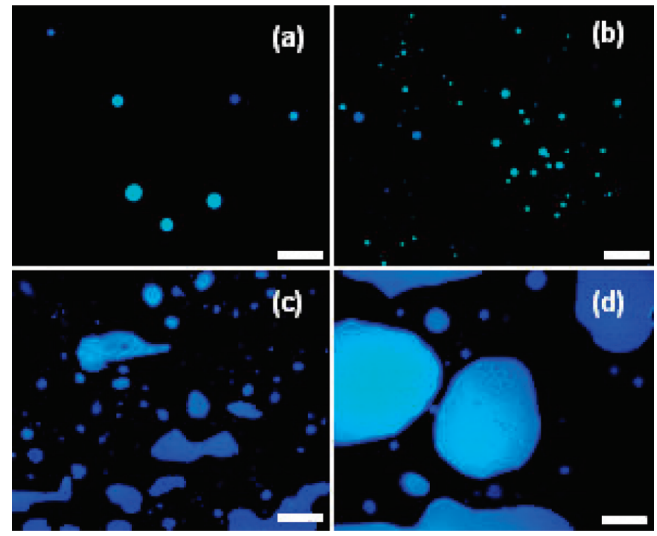

Figure 11. Fluorescence image of L-61 at (a) 1.0; (b) 5.0; (c) 10.0; and (d) 15.0 wt %. Bar = 100 μm. Magnification = 200.

A further increase of L-61 concentration to 1 wt % or above led to the disappearance of the main phase transition peak, indicative of complete disruption of lipid bilayer. Consequently, the measurement of HHW and ΔH cannot be done. Moreover, the sample became cloudy, as opposed to the case of F-127. For 5−15 wt % L-61, only a broad CMT peak was observed in the DSC thermogram as shown in Figure 10. Vesicles were thought to be completely solubilized by L-61 to form mixed micelles. The very short hydrophilic blocks of L-61 on the surfaces of mixed micelles cause the micelles to become less stable in aqueous solution, and hence they tend to aggregate strongly or even precipitate. The interaction and complexation of phospholipid with Pluronic L-61 at low and high concentrations are illustrated in Figure 6. These DSC results shed light on why L-61 at 1 wt % appears very toxic and causes destruction of cells from the prior in vitro experimental study, whereas F-127 shows its ability to maintain cell viability at the same concentration.[43]

We now discuss the results of fluorescence microscopy. Unlike F-127, pure L-61 solutions at 0.3 wt % or above did show DPH fluorescence intensity. The fluorescence became quite prominent when the concentration was 1 wt % or higher as shown in Figure 11. As mentioned earlier, L-61 starts to form crew-cut aggregates at quite low concentrations, due to its strong hydrophobicity. The aggregates can take up DPH and provide an environment that is hydrophobic enough to facilitate the fluorescent emission of DPH. We found from Figure 11 that the aggregates increase in size with increasing concentration and can indeed become very large. This behavior is consistent with the observed turbidity. Figure 12 exhibits the fluorescence images for 0.5 mg/mL of DPPC at various concentrations of

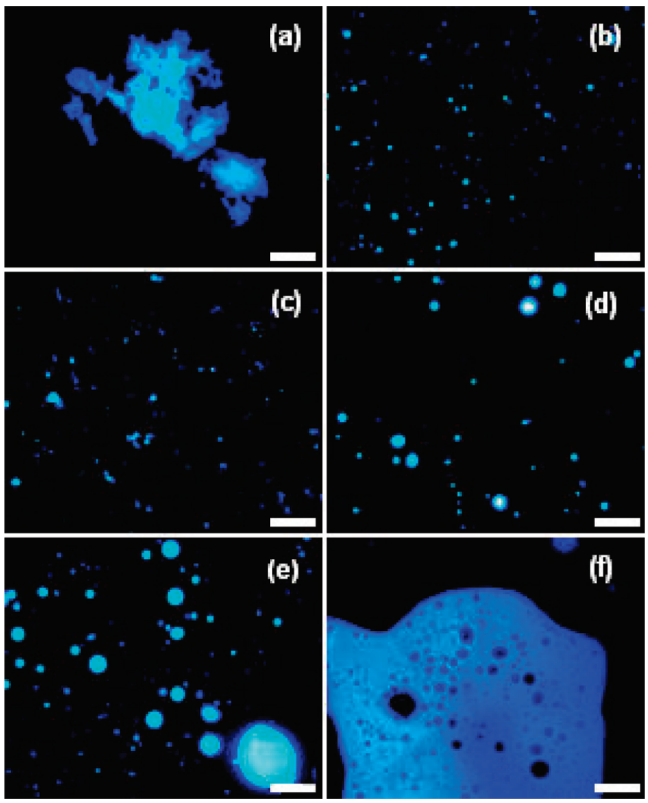

Figure 12. Fluorescence image of DPPC vesicles at different L-61 concentrations: (a) 0.02; (b) 0.3; (c) 0.7; (d) 5.0; (e) 10.0; and (f) 15.0 wt %. Bar = 100 μm. Magnification = 200.

L-61. At 0.02 wt % L-61, the Pluronic disturbs the vesicles strongly, leading to substantial aggregation, in agreement with the DSC result shown earlier. Unlike F-127, L-61 having much shorter hydrophilic blocks is unable to act as a core stabilizer in the unimer state. At 0.3−0.7 wt %, one can see a stark change in the images: instead of huge aggregates, vesicles with expected sizes appeared as usual. These modified vesicles supposedly coexisted with mixed micelles. At higher concentrations (5−15 wt %), very large fluorescent regions emerge in the image, which quite resembles that for L-61 alone. This observation together with the DSC result indicates the dominance of large L-61 crew-cut aggregates that have solubilized DPPC vesicles and disrupted the bilayer structure completely.

4. Conclusions

A comprehensive study on the interaction and complexation between lipid and Pluronic has been conducted using various experimental techniques. The results show a stark difference between F-127 and L-61, although both Pluronic molecules are able to be incorporated in lipid vesicles or solubilize them. Above CMC, the more hydrophilic F-127 forms mixed micelles with lipid molecules, a portion of which can still maintain the bilayer structure as patches. This is clearly evidenced by the nearly identical main transition temperature peak from DSC and a lack of emitting spots from fluorescent microscopy. Also, the bilayer patches remain even when the F-127 undergoes thermal gelation at high enough concentrations. In contrast, the more hydrophobic L-61 disrupts the vesicles more strongly, destroying the bilayer structure eventually when the concentration becomes sufficiently high and thereby leading to the formation of very large, visible aggregates. No main phase transition can be detected any longer. The different behaviors between F-127 and L-61 arise from the distinct length ratios of hydrophilic to hydrophobic block and molecular weights. Our findings can justify why L-61 is toxic to cells and F-127 is superior.

Acknowledgment. The financial support from the National University of Singapore through grant number R-279-000-203-112 is acknowledged.

References and Notes

(1) Kresheck, G. C.; Kale, K.; Vallone, M. D. *J. Colloid Interface Sci.* **1980**, *73*, 460.
(2) Akutsu, H.; Nagamori, T. *Biochemistry* **1991**, *30*, 4510.
(3) Huang, C. *Biochemistry* **1991**, *30*, 26.
(4) Taylor, K. M. G.; Morris, R. M. *Thermochim. Acta* **1995**, *248*, 289.
(5) Wang, G. Q.; Lin, H. N.; Li, S. S.; Huang, C. H. *J. Biol. Chem.* **1995**, *270*, 22738.
(6) Simard, P.; Leroux, J.; Allen, C.; Meyer, O. *Liposome for Drug Delivery*; American Scientific Publishers: CA, 2007.
(7) Woodle, M. C.; Matthav, K. K.; Newman, M. S.; Hadiyat, J. E.; Collins, J. R.; Redemann, C.; Martin, F. J.; Papahadjopoulos, D. *Biochim. Biophys. Acta* **1992**, *1105*, 193.
(8) Litzinger, D. C.; Huang, L. *Biochim. Biophys. Acta* **1992**, *1127*, 249.
(9) Kuhl, T.; Guo, Y.; Alderfer, J. L.; Berman, A. D.; Leckband, D.; Israelachvile, J.; Hui, S. W. *Langmuir* **1996**, *12*, 3003.
(10) Du, H.; Chandaroy, P.; Hui, S. W. *Biochim. Biophys. Acta* **1997**, *1326*, 236.
(11) Mishima, K.; Satoh, K.; Suzuki, K. *Colloid Surf. B* **1997**, *10*, 113.
(12) Hui, S. W.; Kuhl, T. L.; Guo, Y. Q.; Israelachvili, J. *Colloid Surf. B* **1999**, *14*, 213.
(13) Gilbert, J. C.; Richardson, J. L.; Davies, M. C.; Palin, K. J.; Hadgraft, J. *J. Controlled Release* **1987**, *5*, 113.
(14) Chaibundit, C.; Ricardo, N. M. P. S.; Costa, F. M. L. L.; Yeates, S. G.; Booth, C. *Langmuir* **2007**, *23*, 9229.
(15) Kostarelos, K.; Tadros, T. F.; Luckham, P. F. *Langmuir* **1999**, *15*, 369.
(16) Chandaroy, P.; Sen, A.; Hui, S. W. *J. Controlled Release* **2001**, *76*, 27.
(17) Bergstrand, N.; Edwards, K. *J. Colloid Interface Sci.* **2004**, *276*, 400.
(18) Ruysschaert, T.; Sonnen, A. F. P.; Haefele, T.; Meler, W.; Winterhalter, M.; Fournier, D. *J. Am. Chem. Soc.* **2005**, *127*, 6242.
(19) Grassi, G.; Crevatin, A.; Farra, R.; Guarnieri, G.; Pascotto, A.; Rehimers, B.; Lapasin, R.; Grassi, M. *J. Colloid Interface Sci.* **2006**, *301*, 282.
(20) Sabín, J.; Prieto, G.; Blanco, E.; Ruso, J. M.; Angelini, R.; Bordi, F.; Sarmiento, F. *J. Therm. Anal. Calorim.* **2007**, *87*, 199.
(21) Jamshaid, M.; Farr, S. J.; Kearney, P.; Kellaway, I. W. *Int. J. Pharm.* **1988**, *48*, 125.
(22) Woodle, M. C.; Newman, M. S.; Martin, F. J. *Int. J. Pharm.* **1992**, *88*, 327.
(23) Liang, X. M.; Mao, G. Z.; Ng, K. Y. S. *J. Colloid Interface Sci.* **2005**, *285*, 360.
(24) Bochot, A.; Fattal, E.; Gulik, A.; Couarraze, G.; Couvreur, P. *Pharm. Res.* **1998**, *15*, 1364.
(25) Bentley, M. V. L. B.; Marchetti, J. M.; Ricardo, N.; Ali-Abi, Z.; Collett, J. H. *Int. J. Pharm.* **1999**, *193*, 49.
(26) Gaucher, G.; Dufresne, M. H.; Sant, V. P.; Kang, N.; Maysinger, D.; Leroux, J. C. *J. Controlled Release* **2005**, *109*, 169.
(27) Hrubý, M.; Koňák, C.; Ulbrich, K. *J. Controlled Release* **2005**, *103*, 137.
(28) Minko, T.; Batrakova, E. V.; Li, S.; Li, Y.; Pakunlu, R. I.; Alakhov, V. Y.; Kabanov, A. V. *J. Controlled Release* **2005**, *105*, 269.
(29) Soga, O.; Nostrum, C. F.; Fens, M.; Rijcken, C. J. F.; Schiffelers, R. M.; Storm, G.; Hennink, W. E. *J. Controlled Release* **2005**, *103*, 341.
(30) Agrawal, S. K.; Sanabria-Delong, N.; Coburn, J. M.; Tew, G. N.; Bhatia, S. R. *J. Controlled Release* **2006**, *112*, 64.
(31) Batrakova, E. V.; Kabanov, A. V. *J. Controlled Release* **2008**, *130*, 98.
(32) Huh, K. M.; Min, H. S.; Lee, S. C.; Lee, H. J.; Kim, S. W.; Park, K. *J. Controlled Release* **2008**, *126*, 122.
(33) Alakhov, V.; Klinski, E.; Li, S. M.; Pietrzynski, G.; Venne, A.; Batrakova, E.; Bronitch, T.; Kabanov, A. *Colloids Surf. B* **1999**, *16*, 113.
(34) Kabanov, A. V.; Batrakova, E. V.; Alakhov, V. Y. *J. Controlled Release* **2002**, *82*, 189.
(35) Oh, K. T.; Bronich, T. K.; Kabanov, A. V. *J. Controlled Release* **2004**, *94*, 411.
(36) Zhirnov, A. E.; Demina, T. V.; Krylova, O. O.; Grozdova, I. D.; Melik-Nubarov, N. S. *Biochim. Biophys. Acta* **2005**, *1720*, 73.

(37) Alakhov, V.; Moskaleva, E.; Batrakova, E. V.; Kabanov, A. V. *Bioconjugate Chem.* **1996**, *7*, 209.
(38) Kabanov, A. V.; Batrakova, E. V.; Alakhov, V. Y. *Adv. Drug Delivery Rev.* **2002**, *54*, 759.
(39) Batrakova, E. V.; Lee, S.; Li, S.; Venne, A.; Alakhov, V.; Kabanov, A. *Pharm. Res.* **1999**, *16*, 1373.
(40) Krylova, O. O.; Melik-Nubarov, N. S.; Badun, G. A.; Ksenofontov, A. L.; Menger, F. M.; Yaroslavov, A. A. *Chem.—Eur. J.* **2003**, *9*, 3930.
(41) Demina, T.; Grozdova, I.; Krylova, O.; Zhirnov, A.; Istratov, V.; Frey, H.; Kautz, H.; Melik-Nubarov, N. *Biochemistry* **2005**, *44*, 4042.
(42) Erukova, V. Yu.; Krylova, O. O.; Antonenko, N. Y.; Melik-Nubarov, N. S. *Biochim. Biophys. Acta* **2000**, *1468*, 73.
(43) Exner, A. A.; Krupka, T. M.; Scherrer, K.; Teets, J. M. *J. Controlled Release* **2005**, *106*, 188.
(44) Schmolka, I. R. *J. Am. Oil Chem. Soc.* **1977**, *54*, 110.
(45) Alexandridis, P.; Holzwarth, J. F.; Alan Hatton, T. A. *Macromolecules* **1994**, *27*, 2414.
(46) Meulenaer, B. D.; Meeren, P. V.; Cuyper, M. D.; Vanderdeelen, J.; Baert, L. *J. Colloid Interface Sci.* **1997**, *189*, 254.
(47) Šegota, S.; Težak, D. *Adv. Colloid Interface Sci.* **2006**, *121*, 51.
(48) Silvander, M. *Prog. Colloid Polym. Sci.* **2002**, *120*, 35.
(49) Johnsson, M.; Silvander, M.; Karlsson, G.; Edwards, K. *Langmuir* **1999**, *15*, 6314.
(50) Almgren, M. *Biochim. Biophys. Acta* **2000**, *1508*, 146.
(51) Inoue, T.; Yamahata, T.; Shimozawa, R. *J. Colloid Interface Sci.* **1992**, *149*, 345.
(52) Chern, C. S.; Chiu, H. C.; Yang, Y. S. *J. Colloid Interface Sci.* **2006**, *302*, 335.
(53) Lichtenberg, D.; Robson, R. J.; Dennis, E. A. *Biochim. Biophys. Acta* **1983**, *737*, 285.
(54) Lichtenberg, D. *Biochim. Biophys. Acta* **1985**, *821*, 470.
(55) Silvander, M.; Karlsson, G.; Edwards, K. *J. Colloid Interface Sci.* **1996**, *179*, 104.
(56) Kragh-Hansen, U.; Maire, M. L.; Møller, J. V. *Biophys. J.* **1998**, *75*, 2932.
(57) Tan, A.; Ziegler, A.; Steinbauer, B.; Seelig, J. *Biophys. J.* **2002**, *83*, 1547.
(58) Liu, J.; Allen, C. *Polymeric Nanocarriers: Delivery Technology for Therapies of the 21st Century*; PharmaVentures Ltd.: 2003.
(59) Venema, F. R.; Weringa, W. D. *J. Colloid Interface Sci.* **1988**, *125*, 484.
(60) Lasonder, E.; Weringa, W. D. *J. Colloid Interface Sci.* **1990**, *139*, 469.
(61) Fukuda, K.; Ohshima, H.; Kondo, T. *J. Colloid Interface Sci.* **1988**, *123*, 447.
(62) Könczöl, F.; Farkas, N.; Dergez, T.; Belágyi, J.; Lörinczy, D. *J. Therm. Anal. Calorim.* **2005**, *82*, 201.
(63) Pappalardo, M.; Milardi, D.; Grasso, D.; Rosa, C. L. *J. Therm. Anal. Calorim.* **2005**, *80*, 413.
(64) Pantusa, M.; Bartucci, R.; Sportelli, L. *Colloid Polym. Sci.* **2007**, *285*, 649.
(65) Chang, L. C.; Lin, C. Y.; Kuo, M. W.; Gau, C. S. *J. Colloid Interface Sci.* **2005**, *285*, 640.
(66) Chang, L. C.; Chang, Y. Y.; Gau, C. S. *J. Colloid Interface Sci.* **2008**, *322*, 263.

JP906929U